

Concatenated Irregular Variable Length Coding and Irregular Unity Rate Coding

R. G. Maunder and L. Hanzo
Corresponding author: lh@ecs.soton.ac.uk

Abstract—In this contribution we propose the novel serial concatenation of Irregular Variable Length Coding (IrVLC) and Irregular Unity Rate Coding (IrURC), where we matched the corresponding EXtrinsic Information Transfer (EXIT) functions to each other. This approach facilitates a higher degree of design freedom than matching the EXIT function of an irregular codec to that of a regular codec. As a result, a narrow EXIT chart tunnel can be created, facilitating operation at E_b/N_0 values that are closer to the channel's capacity bound. The computational complexity and Bit Error Ratio (BER) performance of our IrVLC-IrURC scheme is favourable in comparison to the benchmark markers that replace either one or both of the irregular codecs by the equivalent-rate regular codec.

I. INTRODUCTION

The serial concatenation [1] and iterative decoding [2] of an irregular outer code with a regular inner code was proposed by Tüchler and Hagenauer in [3]. The irregular outer codec is comprised of a number of component codes, having a variety of coding rates. These different-rate component codes are invoked to generate specific fractions of the encoded bit sequence, which may be specifically chosen in order to shape the EXtrinsic Information Transfer (EXIT) function [4] of the irregular outer code so that it matches that of the regular inner code. This facilitates the creation of an open EXIT chart tunnel [5] and the achievement of iterative decoding convergence to an infinitesimally low probability of error at channel E_b/N_0 values that are close to the channel's capacity bound. Both Irregular Convolutional Codes (IrCCs) [3], [6]–[10] and Irregular Variable Length Codes (IrVLCs) [11]–[15] have been proposed for use as outer irregular codes.

Note that an improved EXIT chart match can be expected if both the outer and inner codes are irregular, since this facilitates a higher degree of design freedom. Hence, in Section II of this paper, we detail the serial concatenation and iterative decoding of an outer IrVLC and a novel inner Irregular Unity Rate Code (IrURC). The joint EXIT chart matching of the irregular codes of this IrVLC-IrURC scheme is discussed in Section III. In Section IV, we compare both the Bit Error Ratio (BER) performance and the computational complexity of the IrVLC-IrURC scheme to those of the benchmark markers that replace either one or both of the irregular codes with the equivalent regular code. Finally, we provide our conclusions in Section V.

The financial support of the EPSRC, Swindon UK and the EU under the auspices of the Optimix project is gratefully acknowledged.

II. OVERVIEW OF THE PROPOSED TRANSMISSION SCHEME

In this section we consider a transmission scheme that facilitates the joint source and channel coding of a sequence of source symbols having values with unequal probabilities of occurrence for near-capacity transmission over an uncorrelated narrowband Rayleigh fading channel. As discussed in [11], this application motivates the employment of an IrVLC outer codec. This is serially concatenated and iteratively decoded by exchanging extrinsic information with a novel IrURC used as the inner codec. Owing to its unity coding rate, the IrURC code facilitates transmission without an effective throughput loss, as suggested in [16].

In the proposed transmission scheme, the outer IrVLC arrangement employs N number of component VLC codebooks $\{\mathbf{VLEC}^n\}_{n=1}^N$ of the Variable Length Error Correction (VLEC) [17] class. These have various coding rates $\{R(\mathbf{VLEC}^n)\}_{n=1}^N$ and/or free distance lower bounds $\{\bar{d}_{\text{free}}(\mathbf{VLEC}^n)\}_{n=1}^N$ [17] and are employed for generating the particular fractions of the encoded bit sequence [11]. Similarly, the inner IrURC arrangement employs M number of component Unity Rate Codes (URC) $\{\mathbf{URC}^m\}_{m=1}^M$ [18], having various generator and/or feedback polynomials. The schematic of the proposed transmission scheme is provided in Figure 1.

A. Joint source and channel coding. We employ $K = 16$ -ary source symbols having values obeying the probabilities of occurrence that result from the Lloyd-Max quantization [19], [20] of independent Gaussian distributed source samples. Note that these occurrence probabilities vary by more than an order of magnitude between 0.0082 and 0.1019 and are given by integrating the Gaussian Probability Density Function (PDF) between each pair of adjacent quantization decision boundaries [19]. These probabilities correspond to between 3.29 and 6.93 bits of information per symbol, motivating the application of VLCs and giving a source entropy of $E = 3.77$ bits/symbol.

In the transmitter shown in Figure 1, the source symbol frame \mathbf{s} is decomposed into N number of components $\{\mathbf{s}^n\}_{n=1}^N$, where each component \mathbf{s}^n comprises J^n number of K -ary source symbols. Hence, the total number of source symbols in the source symbol frame \mathbf{s} is given by $J = \sum_{n=1}^N J^n$. Each of the N number of source symbol frame components $\{\mathbf{s}^n\}_{n=1}^N$ is VLEC-encoded using the corresponding K -entry VLEC codebook from the set $\{\mathbf{VLEC}^n\}_{n=1}^N$, in order to obtain the VLC-encoded bit frame component \mathbf{u}^n , which has a length of I^n bits.

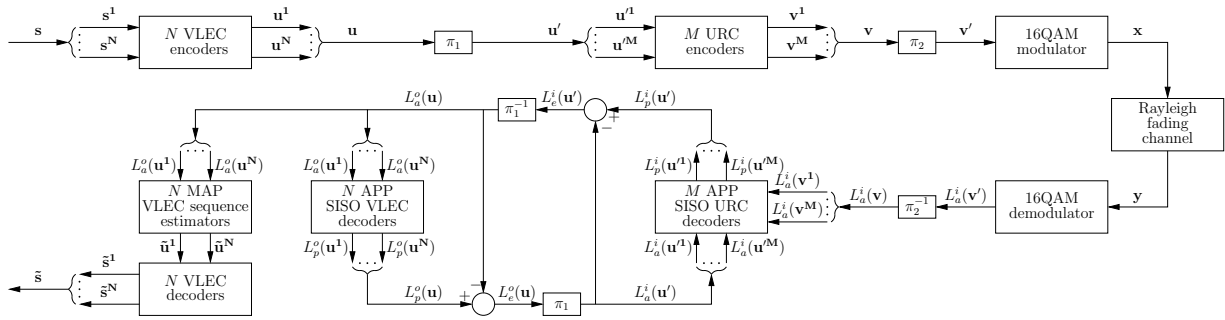


Fig. 1. Schematic of the proposed transmission scheme.

Owing to the variable lengths of the VLEC codewords, the VLC-encoded bit frame component lengths $\{I^n\}_{n=1}^N$ will typically vary from frame to frame. In order to facilitate the VLEC decoding of the VLC-encoded bit frame components $\{u^n\}_{n=1}^N$, it is necessary to explicitly convey their lengths $\{I^n\}_{n=1}^N$ to the receiver. Furthermore, this highly error sensitive side information must be reliably protected against transmission errors, using a powerful low rate block code, for example. For the sake of avoiding obfuscation, this is not shown in Figure 1. Note that since the amount of the encoded side information is typically negligible compared to the length of the VLC-encoded bit frame components $\{u^n\}_{n=1}^N$ [11], we do not consider it any further in this paper.

In the scheme's transmitter, the N number of VLC-encoded bit frame components $\{u^n\}_{n=1}^N$ are concatenated. As shown in Figure 1, the resultant VLC-encoded bit frame u has a length of $I = \sum_{n=1}^N I^n$ bits, where I will typically vary from frame to frame. Note that the average fractions I^n/I of the VLC-encoded bit frame u that are generated by each VLEC component code VLEC^n may be chosen in order to shape the inverted EXIT function of the IrVLC code [3], as will be detailed in Section III. The corresponding fractions J^n/J of the source symbol frame s that should be encoded by each VLEC component code VLEC^n may be obtained as $J^n/J = I^n/I \cdot R(\text{VLEC}^n)/R_{VLC}$, where R_{VLC} is the overall outer coding rate.

In the transmitter shown in Figure 1, the VLC-encoded bit frame u is interleaved using a random I -bit interleaver π_1 in order to obtain the interleaved VLC-encoded bit frame u' . This is decomposed into M number of components $\{u'^m\}_{m=1}^M$, where each component u'^m comprises I^m number of bits. Note that the fractions $\{I^m/I\}_{m=1}^M$ may be chosen in order to shape the EXIT function of the IrURC codec [3], as will be detailed in Section III. Each of the M number of interleaved VLC-encoded bit frame components $\{u'^m\}_{m=1}^M$ is URC-encoded using the corresponding URC from the set $\{\text{URC}^m\}_{m=1}^M$. Since all URCs have a coding rate of unity, the resultant URC-encoded bit frame components $\{v^m\}_{m=1}^M$ have the same lengths as the corresponding interleaved VLC-encoded bit frame components $\{u'^m\}_{m=1}^M$ and the overall inner coding rate will be $R_{URC} = 1$. As shown in Figure 1, the URC-encoded bit frame components $\{v^m\}_{m=1}^M$

are concatenated to provide the URC-encoded bit frame v , having a length of I number of bits. Finally, this frame is interleaved using a random I -bit interleaver π_2 , modulated using Gray-mapped $M_{QAM} = 16$ -ary Quadrature Amplitude Modulation (16QAM) [21] and transmitted over the Rayleigh fading channel, as shown in Figure 1.

B. Iterative decoding. In the receiver, *A Posteriori Probability* (APP) Soft-In Soft-Out (SISO) IrURC- and IrVLC-decoding are performed iteratively, as shown in Figure 1. Both of these decoders invoke the Bahl-Cocke-Jelinek-Raviv (BCJR) algorithm [22] applied to the bit-based trellises [23]–[25]. All BCJR calculations are performed in the logarithmic probability domain and using an eight-entry lookup table for correcting the Jacobian approximation [26]. Note that this approach requires only the use of Add, Compare and Select (ACS) operations. The extrinsic soft information, represented in the form of Logarithmic Likelihood Ratios (LLRs) [24], is iteratively exchanged between the IrURC and IrVLC decoding stages for the sake of assisting each other's operation as usual and as detailed in [1], [2]. Following the final decoding iteration, bit-based Maximum *A Posteriori* (MAP) VLEC sequence estimation is performed as usual [11]. In Figure 1, $L(\cdot)$ denotes the LLRs of the bits concerned, where the superscript i indicates inner IrURC decoding, while o corresponds to outer IrVLC decoding. Additionally, a subscript denotes the dedicated role of the LLRs, with a , p and e indicating *a priori*, *a posteriori* and extrinsic information, respectively. Similarly, a tilde over the notation represents a reconstructed estimate of the bits or symbols concerned.

Just as N and M number of separate VLEC and URC encoding processes are employed in the proposed transmission scheme's transmitter, respectively, N and M number of separate VLEC and URC decoding processes are employed in its receiver, respectively. Furthermore, in parallel to the operation of the encoding processes on the basis of subframes of bits or symbols, the decoding processes operate on the basis of subframes of LLRs or reconstructed bit or symbol estimates, as shown in Figure 1. Note that the decomposition of the *a priori* LLR frame $L_a^o(u)$ into N number of components is performed with the aid of the explicit side information that conveys the number of bits I^n in each VLC-encoded bit frame component u^n .

III. SYSTEM PARAMETER DESIGN

In this section we introduce three different parameterisations of the proposed transmission scheme of Section II. We refer to these as the IrVLC-IrURC, the IrVLC-URC, and the VLC-URC parameterisations. Note that in all cases, an outer coding rate of $R_{VLC} = 0.53$ is employed, yielding an effective throughput of $\eta = R_{VLC} \cdot R_{URC} \cdot \log_2(M_{QAM}) = 2.12$ bits per channel use, which corresponds to the Rayleigh fading channel capacity bound of 4.3 dB [21].

In the IrVLC-IrURC and IrVLC-URC parameterisations, $N = 30$ component VLEC codebooks $\{\mathbf{VLEC}^n\}_{n=1}^{30}$ are employed, as described in Section II. These were designed using a genetic algorithm to have a range of coding rates $\{R(\mathbf{VLEC}^n)\}_{n=1}^{30}$ and free distance lower bounds $\{\bar{d}_{\text{free}}(\mathbf{VLEC}^n)\}_{n=1}^{30}$. In all cases, free distance lower bounds of at least two were sought, since this was found to yield inverted EXIT functions that reach the (1, 1) unity information point of the EXIT chart, as shown in Figure 2. For each considered VLEC codebook VLEC, both the coding rate $R(\mathbf{VLEC})$ and the free distance lower bound $\bar{d}_{\text{free}}(\mathbf{VLEC})$ is provided in Figure 2.

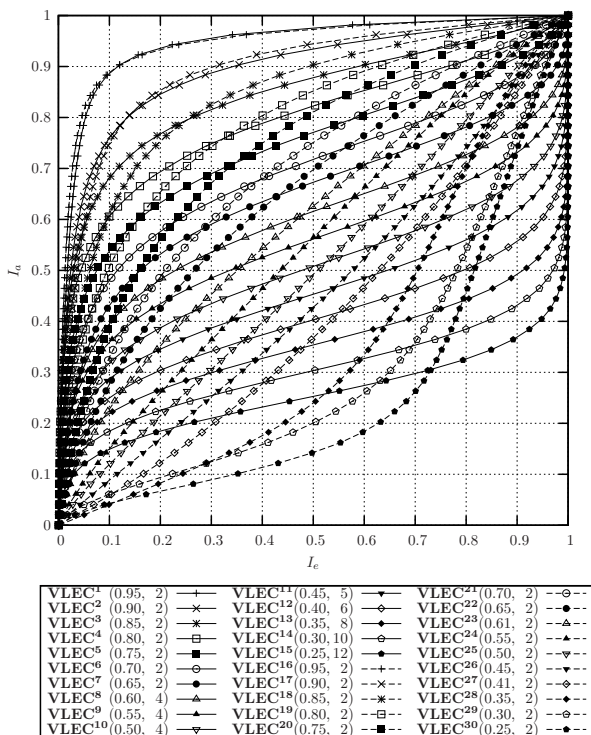


Fig. 2. Inverted EXIT functions for the $N = 30$ component VLEC codebooks $\{\mathbf{VLEC}^n\}_{n=1}^{30}$. Curves are labelled using the format $\mathbf{VLEC}(R(\mathbf{VLEC}), \bar{d}_{\text{free}}(\mathbf{VLEC}))$.

By contrast, in the VLC-URC parameterisation, just $N = 1$ component VLEC codebook is employed, representing a regular VLC arrangement. This component codebook was designed using a genetic algorithm to have a free distance lower bound of 4, which was the highest that was achievable for the above-mentioned coding rate of 0.53. The inverted

EXIT function of the VLC-URC parameterisation's VLEC codebook is portrayed in Figure 4.

In the IrVLC-IrURC parameterisation, $M = 10$ component URC codes $\{\mathbf{URC}^m\}_{m=1}^{10}$ having different generator and/or feedback polynomials are employed, as described in Section II. By contrast, in the IrVLC-URC and VLC-URC parameterisations, only $M = 1$ component URC code is employed, namely \mathbf{URC}^1 . The $M = 10$ component URC codes $\{\mathbf{URC}^m\}_{m=1}^{10}$ were selected from the set of all possible URC code designs that have shift register representations containing no more than three memory elements in order to yield a wide variety of EXIT function shapes, as seen for the channel's E_b/N_0 capacity bound of 4.3 dB in Figure 3. Both the generator and feedback polynomials of the component URC codes $\{\mathbf{URC}^m\}_{m=1}^{10}$ are shown in Figure 3. Note that some URC component EXIT functions emerge from the (0, 0) point of the EXIT chart, whilst others offer some non-zero extrinsic information even in the absence of any *a priori* information.

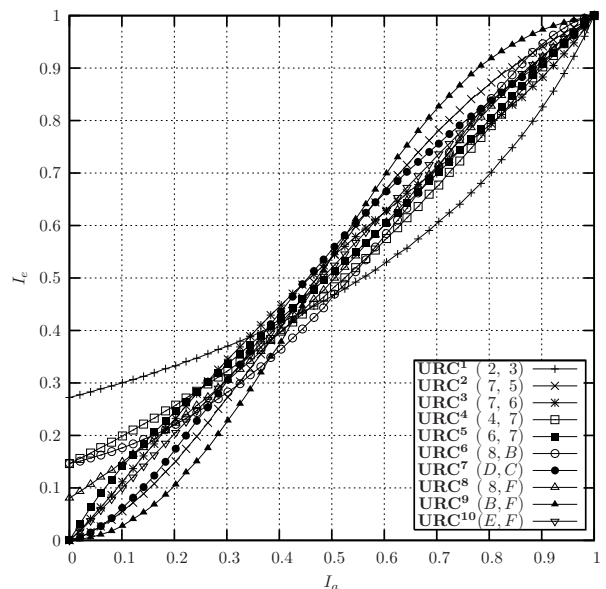


Fig. 3. EXIT functions for the $M = 10$ component URC codes $\{\mathbf{URC}^m\}_{m=1}^{10}$ for a 16QAM-modulated Rayleigh fading channel E_b/N_0 of 4.3 dB and an effective throughput of $\eta = 2.12$ bits per channel use. Curves are labelled using the format $\mathbf{URC}(g(\mathbf{URC}), f(\mathbf{URC}))$, where $g(\mathbf{URC})$ and $f(\mathbf{URC})$ are the hexadecimal generator and feedback polynomials of the URC code, respectively [26].

Ignoring the effects of capacity loss, our scheme's effective throughput of 2.12 bits per channel use is the maximum that can be reliably achieved for 16QAM transmission over an uncorrelated Rayleigh fading channel having an E_b/N_0 value of 4.3 dB [21], as described above. The capacity loss at this E_b/N_0 value of 4.3 dB can be estimated by considering the EXIT functions of Figure 3. More specifically, the attainable capacity for an E_b/N_0 value of 4.3 dB can be estimated [16] by multiplying the average area beneath the EXIT functions of Figure 3 by $\log_2(M_{QAM}) = 4$. This yields an attainable capacity of 2.06 bits per channel use, which is less than the

capacity of 2.12 bits per channel use. It was found that an attainable channel capacity of 2.12 bits per channel use is only achieved for a channel E_b/N_0 value of 4.6 dB, which we refer to as our channel's *attainable* capacity bound.

In the case of the VLC-URC parameterisation, an open EXIT chart tunnel and iterative decoding convergence to an infinitesimally low probability of error are only facilitated for channel E_b/N_0 values in excess of a threshold at 6 dB, as shown in Figure 4. The EXIT chart matching algorithm of [3] was employed to shape the inverted IrVLC EXIT function of the IrVLC-URC parameterisation. In this case, an E_b/N_0 value of 5.1 dB was the threshold at which the inverted IrVLC EXIT function could be matched to the URC EXIT function in order to maintain an open EXIT chart tunnel, as shown in Figure 4. In the case of the IrVLC-IrURC parameterisation, the EXIT chart matching algorithm of [3] was iteratively employed to alternately match the inverted IrVLC EXIT function to the IrURC EXIT function and vice versa. In this case, an E_b/N_0 value of 4.7 dB was the threshold at which an open EXIT chart tunnel could be achieved, as shown in Figure 4.

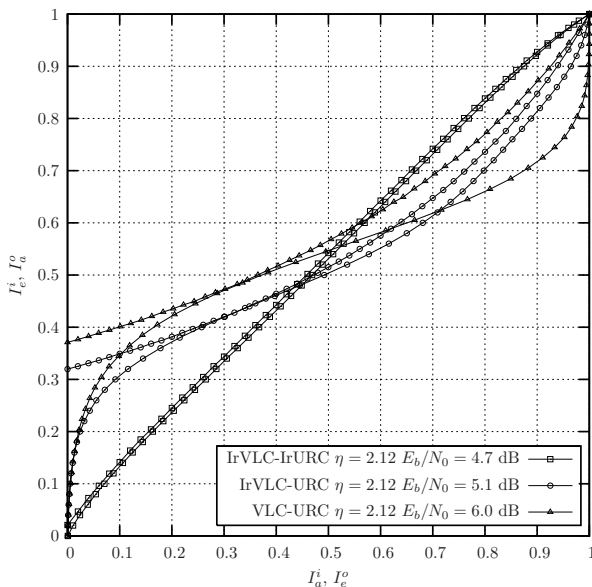


Fig. 4. Inner and inverted outer EXIT functions for the IrVLC-IrURC, IrVLC-URC and VLC-URC parameterisations. Inner EXIT functions are provided for the threshold E_b/N_0 value at which an open EXIT chart tunnel could be achieved.

The threshold E_b/N_0 values of the IrVLC-IrURC, IrVLC-URC and VLC-URC parameterisations are within 0.4 dB, 0.8 dB and 1.7 dB of the channel's capacity bound, respectively. Furthermore, the channel's *attainable* capacity bound is within 0.1 dB, 0.5 dB and 1.4 dB of the threshold E_b/N_0 values of the IrVLC-IrURC, IrVLC-URC and VLC-URC parameterisations, respectively. These discrepancies are commensurate with the area between each parameterisation's inner and inverted outer EXIT functions, owing to the area property of EXIT charts [16]. As may be observed in Figure 4, the inner and inverted outer EXIT functions of the IrVLC-IrURC

parameterisation are near-parallel, having an open EXIT tunnel which is narrow all along its length. By contrast, the inner and inverted outer EXIT functions of the IrVLC-URC and VLC-URC parameterisations are not parallel, having open EXIT tunnels which become narrow only in the vicinity of a specific point along their length. Note that much of the open EXIT chart area between the inner and inverted outer EXIT functions of the IrVLC-URC and VLC-URC parameterisations is a consequence of their URCs' high EXIT chart starting points of (0, 0.32) and (0, 0.37), respectively. By contrast, in the case of the IrVLC-IrURC-high and IrVLC-IrURC-low parameterisations, the presence of the URC component codes that emerge from the (0, 0) point of the EXIT chart facilitates the design of an IrURC scheme having an EXIT function that starts close to this point.

IV. RESULTS

In this section, the achievable performance of the IrVLC-IrURC, the IrVLC-URC and the VLC-URC parameterisations of Section III is characterised and our quantitative findings are presented. In each case two source symbol frame lengths were considered. More specifically, in one of the cases we simulated the transmission of 20 frames of $J = 140\ 640$ randomly generated symbols, which corresponds to an average interleaver length of $I = JE/R \approx 1\ 000\ 000$ bits. By contrast, a shorter source symbol frame length was employed in the other case, in which the transmission of 200 frames of $J = 14\ 064$ symbols was simulated, corresponding to an average interleaver length of $I \approx 100\ 000$ bits. After each iteration of decoding each frame, we recorded the Bit Error Ratio (BER) that was associated with the VLC-encoded bit frame estimate $\hat{\mathbf{u}}$, together with the cumulative number of ACS operations performed per source symbol so far during iterative decoding. These values were averaged across the frames and the average number of ACS operations per source symbol required to achieve a BER of 10^{-5} at each E_b/N_0 value considered was found. In Figure 5, these computational complexities are plotted against E_b/N_0 for each average interleaver length and each of the IrVLC-IrURC, the IrVLC-URC and the VLC-URC parameterisations.

Observe in Figure 5 that, upon employing the longer average interleaver length of $I \approx 1\ 000\ 000$ bits, the IrVLC-IrURC, the IrVLC-URC and the VLC-URC parameterisations can achieve a BER of less than 10^{-5} for E_b/N_0 values in excess of 4.7 dB, 5.2 dB and 6 dB, which agrees with the EXIT chart analysis of Section III. Naturally, the BER performance is degraded, when the shorter interleaver length of $I \approx 100\ 000$ bits is employed, owing to its poorer mitigation of the correlation within the *a priori* LLR frames $L_a^o(\mathbf{u})$ and $L_a^i(\mathbf{u}')$. As a result, the EXIT chart tunnel is narrowed and iterative decoding convergence to an infinitesimally low BER will be prevented, when the EXIT chart's tunnel closes [5].

As may be expected, operation at lower E_b/N_0 values is associated with a higher computational complexity, owing to the increased number of decoding iterations that are required to 'navigate' through the narrowed EXIT chart tunnel. With

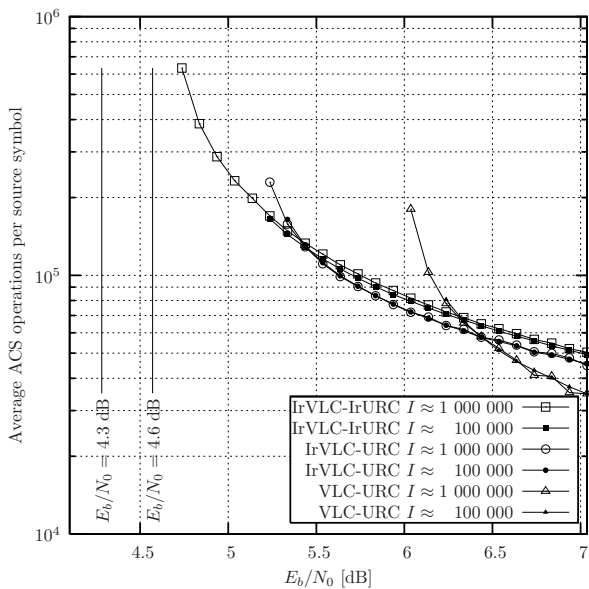


Fig. 5. Average number of ACS operations per source symbol required for the various parameterisations of the proposed transmission scheme to achieve a BER of 10^{-5} when communicating over a 16QAM-modulated Rayleigh fading channel having a range of E_b/N_0 values.

reference to Figure 5, we can identify the IrVLC-IrURC parameterisation as our preferred arrangement, since it allows operation at low E_b/N_0 values that approach the capacity bounds and because it only demands a slightly increased computational complexity than the bench markers at high E_b/N_0 values.

V. CONCLUSIONS

In this paper we have proposed the novel serial concatenation of IrVLC and IrURC, which have jointly matched EXtrinsic Information Transfer (EXIT) functions. This approach facilitates a higher degree of design freedom than matching the EXIT function of an irregular codec to that of a regular codec. As a result, a narrow EXIT chart tunnel can be created, facilitating operation at E_b/N_0 values that are closer to the channel's capacity bound. Indeed, we demonstrated operation within 0.4 dB of the Rayleigh fading channel's capacity limit and within 0.1 dB of the achievable capacity limit. Additionally, gains of 0.5 dB and 1.3 dB were offered over identical-rate IrVLC-URC and VLC-URC bench markers. The computational complexity of these schemes was compared and the IrVLC-IrURC scheme was identified as our preferred arrangement.

REFERENCES

- [1] S. Benedetto and G. Montorsi, "Serial concatenation of block and convolutional codes," *Electronics Letters*, vol. 32, no. 10, pp. 887–888, 1996.
- [2] —, "Iterative decoding of serially concatenated convolutional codes," *Electronics Letters*, vol. 32, no. 13, pp. 1186–1188, 1996.
- [3] M. Tüchler and J. Hagenauer, "EXIT charts of irregular codes," in *Conference on Information Sciences and Systems*, Princeton, NJ, March 2002, pp. 748–753.
- [4] S. ten Brink, "Convergence of iterative decoding," *Electronics Letters*, vol. 35, no. 10, pp. 806–808, 1999.

- [5] A. Ashikhmin, G. Kramer, and S. ten Brink, "Extrinsic information transfer functions: model and erasure channel properties," *IEEE Transactions on Information Theory*, vol. 50, no. 11, pp. 2657–2673, November 2004.
- [6] M. Tüchler, "Design of serially concatenated systems depending on the block length," *IEEE Transactions on Communications*, vol. 52, no. 2, pp. 209–218, February 2004.
- [7] J. Wang, S. X. Ng, A. Wolfgang, L.-L. Yang, S. Chen, and L. Hanzo, "Near-capacity three-stage MMSE turbo equalization using irregular convolutional codes," in *International Symposium on Turbo Codes*, Munich, Germany, April 2006, electronic publication.
- [8] A. Q. Pham, J. Wang, L.-L. Yang, and L. Hanzo, "An Iterative Detection Aided Unequal Error Protection Wavelet Video Scheme Using Irregular Convolutional Codes," in *IEEE Vehicular Technology Conference*, vol. 5, 2006, pp. 2484–2488.
- [9] O. Alamri, J. Wang, S. X. Ng, L.-L. Yang, and L. Hanzo, "Near-Capacity Three-Stage Turbo Detection of Irregular Convolutional Coded Joint Sphere-Packing Modulation and Space-Time Coding," in *Proceedings of the IEEE International Communications Conference*, Glasgow, UK, June 2007.
- [10] J. Wang, N. S. Othman, J. Kliewer, L.-L. Yang, and L. Hanzo, "Turbo-detected unequal error protection irregular convolutional codes designed for the wideband advanced multirate speech codec," in *IEEE Vehicular Technology Conference*, vol. 2, Sept. 2005, pp. 927–931.
- [11] R. G. Maunder, J. Wang, S. X. Ng, L.-L. Yang, and L. Hanzo, "Iteratively Decoded Irregular Variable Length Coding and Trellis Coded Modulation," in *IEEE Workshop on Signal Processing Systems*, Shanghai, China, October 2007. [Online]. Available: <http://www.ecs.soton.ac.uk/people/rm02r>
- [12] —, "On the Performance and Complexity of Irregular Variable Length Codes for Near-Capacity Joint Source and Channel Coding," accepted for publication by *IEEE Transactions on Wireless Communications*.
- [13] S. Ahmed, R. G. Maunder, L.-L. Yang, S. X. Ng, and L. Hanzo, "Joint Source Coding, Unity Rate Precoding and FFH-MFSK Modulation using Iteratively Decoded Irregular Variable Length Coding," in *IEEE Vehicular Technology Conference*, Baltimore, USA, September 2007.
- [14] M. El-Hajjar, R. G. Maunder, O. Alamri, S. X. Ng, and L. Hanzo, "Iteratively Decoded Irregular Variable Length Coding and Sphere-Packing Modulation-Aided Differential Space-Time Spreading," in *IEEE Vehicular Technology Conference*, Baltimore, USA, September 2007.
- [15] R. G. Maunder and L. Hanzo, "Genetic Algorithm Aided Design of Variable Length Error Correcting Codes for Arbitrary Coding Rate and Error Correction Capability," submitted to *IEEE Transactions on Communications*.
- [16] A. Ashikhmin, G. Kramer, and S. ten Brink, "Code rate and the area under extrinsic information transfer curves," in *IEEE International Symposium on Information Theory*, 2002.
- [17] V. Buttigieg and P. G. Farrell, "Variable-length error-correcting codes," *IEE Proceedings on Communications*, vol. 147, no. 4, pp. 211–215, August 2000.
- [18] D. Divsalar, S. Dolinar, and F. Pollara, "Serial concatenated trellis coded modulation with rate-1 inner code," in *IEEE Global Telecommunications Conference*, vol. 2, San Francisco, CA, USA, 2000, pp. 777–782.
- [19] S. Lloyd, "Least squares quantization in PCM," *IEEE Transactions on Information Theory*, vol. 28, no. 2, pp. 129–137, 1982.
- [20] J. Max, "Quantizing for minimum distortion," *IRE Transactions on Information Theory*, vol. 6, no. 1, pp. 7–12, March 1960.
- [21] L. Hanzo, S. X. Ng, T. Keller, and W. Webb, *Quadrature Amplitude Modulation*. Chichester, UK: Wiley, 2004.
- [22] L. Bahl, J. Cocke, F. Jelinek, and J. Raviv, "Optimal decoding of linear codes for minimizing symbol error rate (Corresp.)," *IEEE Transactions on Information Theory*, vol. 20, no. 2, pp. 284–287, 1974.
- [23] V. B. Balakirsky, "Joint source-channel coding with variable length codes," in *IEEE International Symposium on Information Theory*, Ulm, Germany, June 1997, p. 419.
- [24] R. Bauer and J. Hagenauer, "On variable length codes for iterative source/channel decoding," in *Data Compression Conference*, Snowbird, UT, March 2001, pp. 273–282.
- [25] G. D. Forney, "Review of random tree codes," NASA Ames Research Center, Moffett Field, CA, USA, Tech. Rep. NASA CR73176, December 1967.
- [26] L. Hanzo, T. H. Liew, and B. L. Yeap, *Turbo Coding, Turbo Equalisation and Space Time Coding for Transmission over Wireless Channels*. Chichester, UK: Wiley, 2002.